Materials Science Research International, Vol.5, No.3 pp.195-201 (1999)

General paper

COMPUTER SIMULATION METHOD FOR CRACK GROWTH USING INTERFACE ELEMENT EMPLOYING LENNARD-JONES TYPE POTENTIAL FUNCTION

Hidekazu MURAKAWA and Zhengqi WU

Joining and Welding Research Institute, Osaka University, 11-1 Mihogaoka, Ibaraki, Osaka 567-0047, Japan

Abstract: The phenomena of crack propagation and interface debonding can be regarded as formation of new surface. Thus, it is quite natural to model these problems by introducing the mechanism of surface formation. The authors proposed a method in which the formation of new surface is represented by interface element based on the interface potential energy. The general idea of the interface element and its application to peeling test of bonded plates, push-out test of fiber in matrix, dynamic crack propagation and ductile tearing of steel plate are presented.

Key words: *Interface Element, Interface Potential, Peeling Test, Push-out Test, Dynamic Crack Propagation, Ductile Crack Propagation*

1. INTRODUCTION

Fiber reinforced composite materials and the composites with a thin film coating are applied in various fields as the structural materials because of their high specific strength and stiffness which are effective for weight savings. The conventional materials, such as metals and ceramics, are also used under severe conditions due to the recent improvement of their performances. From the point of view of safety design of structures, it is very important to estimate the fracture strength of materials with a reasonable accuracy. Many methods for evaluating the failure strength of materials have been proposed. There are basically two approaches. One is the macroscopic approach in which the concepts of stress intensity factor, energy release rate and J-integral are employed. The other is the microscopic approach such as the simulations of crack propagation using the molecular dynamics [1]. To evaluate the strength of structural component, both the macroscopic and the microscopic nature of the phenomena must be taken into account [2-4].

In this study, a new and simple method is developed in order to simulate the fracture phenomena that can be considered as the formation of new surface with the crack propagation [5]. Based on the fact that surface energy must be supplied for the formation of new surface, a potential function representing the surface energy density is introduced in the finite element method(FEM). The proposed method is applied to simple mode-I and II crack propagation problems and its capability for static and dynamic analyses is demonstrated.

2. METHOD OF ANALYSIS

2.1. Surface Potential

Figure 1 shows an illustration of the crack propagation modeled using interface elements. The interface element consists of two surfaces and has no thickness when the load is not acting. When the load is applied, the two surfaces separate from each other. The distance between the surfaces, or the crack opening, is denoted by δ. The mechanical characteristics of the interface element are defined through a potential function $\phi(\delta)$. Since the function $\phi(\delta)$ can be chosen rather arbitrarily, the Lennard-Jones type potential energy [6] described by the following equation is employed in this study.

$$\phi(\delta)=2\gamma\left\{\left(\frac{r_0}{r_0+\delta}\right)^{2n}-2\left(\frac{r_0}{r_0+\delta}\right)^{n}\right\} \tag{1}$$

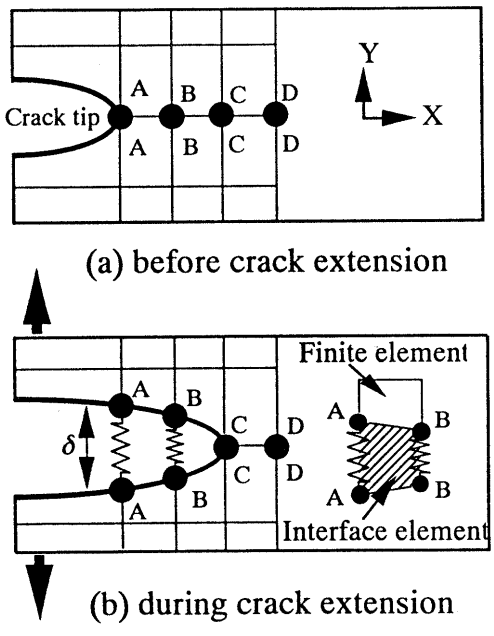

Fig.1. Crack propagation model with interface element.

Received December 10, 1998
Accepted August 12, 1999

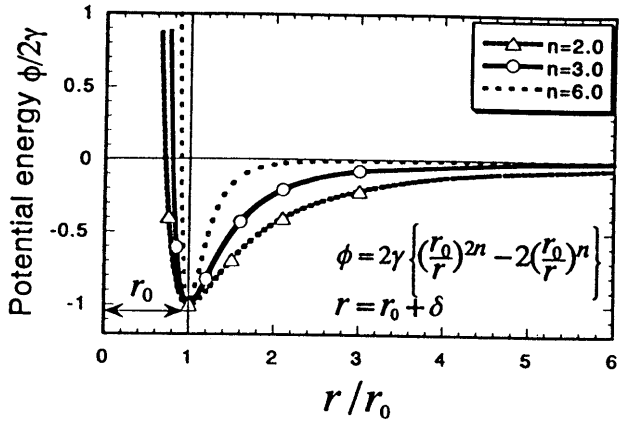

Fig. 2. Lennard-Jones type interface potential.

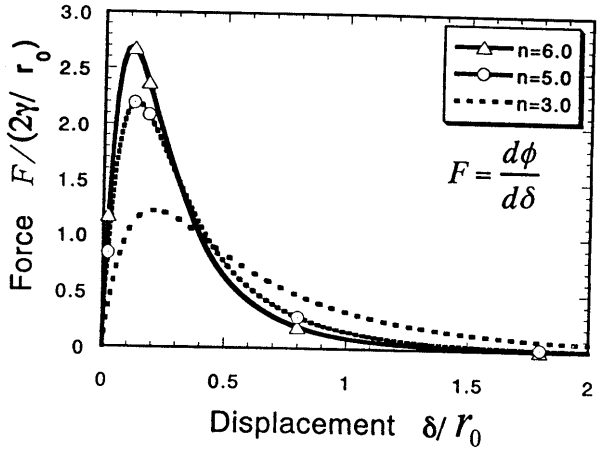

Fig. 3. Bonding force acting on interface.

where δ is the crack opening and γ, n and r_0 are the material constants. Especially, 2γ is the surface energy per unit area. As shown in Fig. 2, n controls the shape of potential energy. The derivative of ϕ with respect to δ gives the bonding force per unit area of the surface. As shown in Fig. 3, the bonding force rapidly decreases with increasing δ. Through this phenomenon, the formation of new surface can be described.

2.2. Equilibrium Equation of System

For simplicity, the outline of the mathematical formulation is presented using the crack propagation problem in elastic solid. When the material is elastic, the equilibrium equation can be derived based on the principle of minimum potential energy.

The total energy Π of the elastic body with propagating crack can be described as the sum of the strain energy U, the potential of external load W and the interface energy for the newly formed surface during crack propagation U_s, i.e.

$$\Pi = U + U_s + W. \tag{2}$$

In case of the finite element method, the elastic body to be analyzed is subdivided into small elements and the displacements in each element are interpolated by nodal displacement u_0. Noting this, the total energy is described as,

$$\Pi = \Pi(u_0) = U(u_0) + U_s(u_0) + W(u_0), \tag{3}$$

Further, $U(u_0)$, $U_s(u_0)$ and $W(u_0)$ can be represented as the sum of the contributions from each element $U^e(u^e_0)$, $U^e_s(u^e_0)$ and $W(u^e_0)$, i.e.

$$\Pi(u_0) = \Sigma\{U^e(u^e_0) + U^e_s(u^e_0) + W(u^e_0)\}, \tag{4}$$

where u^e_0 is the nodal displacement vector for each element extracted from the nodal displacement vector of the whole system u_0.

Once the total energy Π is given as in Eq. (4), the equilibrium equation in incremental form can be derived in the following manner. Denoting the nodal displacement at the present step and its increment to the next step as u_0 and Δu_0, the total energy Π can be described as a function of $u_0 + \Delta u_0$ and it can be expanded into Taylor's series, i.e.

$$\begin{aligned}\Pi(u_0+\Delta u_0) &\cong \Pi(u_0) + \Delta^1\Pi(\Delta u_0) + \Delta^2\Pi(\Delta u_0) \\ &= \Pi(u_0) - \{\Delta u_0\}^T\{f\} + \frac{1}{2}\{\Delta u_0\}^T[k]\{\Delta u_0\},\end{aligned} \tag{5}$$

where $\Delta^1\Pi$ and $\Delta^2\Pi$ are the first and the second terms in Δu_0, i.e.

$$\Delta^1\Pi(u_0) = -\{\Delta u_0\}^T\{f\} \tag{6}$$

$$\Delta^2\Pi(u_0) = \frac{1}{2}\{\Delta u_0\}^T[k]\{\Delta u_0\}. \tag{7}$$

Further, the equilibrium equation can be derived as the stationary condition of $\Pi(u_0+\Delta u_0)$ with respect to Δu_0, i.e.

$$\partial\,\Pi(u_0 + \Delta u_0)/\partial\Delta u_0 = -\{f\} + [k]\{\Delta u_0\}, \tag{8}$$

or,

$$[k]\{\Delta u_0\} = \{f\}. \tag{9}$$

where $[k]$ and $\{f\}$ are the tangent stiffness matrix and the load vector, respectively.

2.3. Stiffness Matrix and Force Vector of Interface Element

The stiffness matrix and the load vector of the interface

element can be derived in the manner basically same as that for the whole system. Since the FEM code developed in this research is a three dimensional one using solid element, the same 8-node solid element is used for the inteface element as shown in Fig. 4. The interface element consists of two surfaces containing four nodes, namely nodes 1-4 for bottom surface and 5-8 for top surface, and it has no thickness when load is not applied. The two surfaces separate when the load is applied and the distance or the opening is denoted by δ. When the surface area of the interface element is S^e, the interface energy for an element $U^e{}_s(u^e{}_0)$ is given by the following equation.

$$U^e{}_s(u^e{}_0) = \int \phi(\delta) \mathrm{d}S^e \ , \tag{10}$$

where δ is the opening at arbitrary point on the surface and it can be interpolated using interpolation function $N_i(\xi, \eta)$, i.e.

$$\delta(\xi,\eta) = \Sigma N_i(\xi,\eta)(w_{i+4} - w_i) \ , \tag{11}$$

where

$$\begin{aligned} N_1(\xi,\eta) &= 0.25(1+\xi)(1-\eta) \\ N_2(\xi,\eta) &= 0.25(1+\xi)(1+\eta) \\ N_3(\xi,\eta) &= 0.25(1-\xi)(1+\eta) \\ N_4(\xi,\eta) &= 0.25(1-\xi)(1-\eta), \end{aligned} \tag{12}$$

and w_i is the nodal displacement normal to the surface.

Finally, the tangent stiffness matrix $[k^e]$ and the load vector $\{f^e\}$ of the interface element can be derived by expanding $U^e{}_s(u^e{}_0 + \Delta u^e{}_0)$ with respect to $\Delta u^e{}_0$ in the following manner.

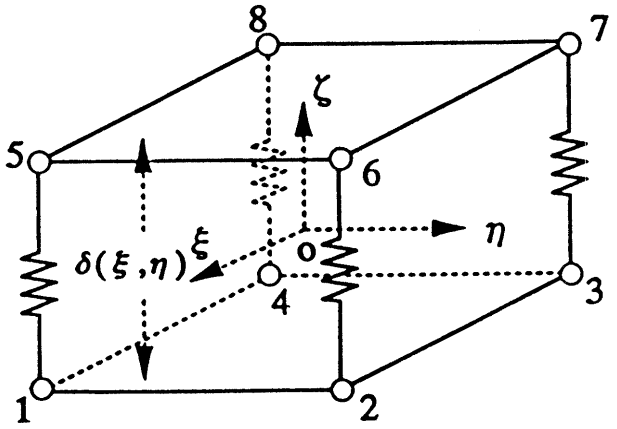

Fig. 4. Interface element and interpolation of crack opening.

$$\begin{aligned} U^e{}_s(u^e{}_0 + \Delta u^e{}_0) &= \int \phi(\delta + \Delta\delta) \mathrm{d}s^e \\ &= \int \phi(\delta) \mathrm{d}s^e + \int \frac{\mathrm{d}\phi(\delta)}{\mathrm{d}\delta} \frac{\partial \delta}{\partial u^e{}_0} \Delta u^e{}_0 \mathrm{d}s^e \\ &\quad + \frac{1}{2} \int \frac{\mathrm{d}^2\phi(\delta)}{\mathrm{d}\delta^2} \left(\frac{\partial \delta}{\partial u^e{}_0} \Delta u^e{}_0 \right)^2 \mathrm{d}s^e + H.O.T. \end{aligned} \tag{13}$$

where

$$\int \frac{\mathrm{d}\phi(\delta)}{\mathrm{d}\delta} \frac{\partial \delta}{\partial u^e{}_0} \Delta u^e{}_0 \mathrm{d}s^e = -\{f^e\}^T \{\Delta u^e{}_0\} \tag{14}$$

$$\begin{aligned} &\frac{1}{2} \int \frac{\mathrm{d}^2\phi(\delta)}{\mathrm{d}\delta^2} \left(\frac{\partial \delta}{\partial u^e{}_0} \Delta u^e{}_0 \right)^2 \mathrm{d}s^e \\ &\qquad = \frac{1}{2} \{\Delta u^e{}_0\}^T [k^e] \{\Delta u^e{}_0\} . \end{aligned} \tag{15}$$

Since the interface element has no volume or mass, the same formulation can be applied to both the static and the dynamic problems. Further, by arranging the interface elements along the crack extension path in the ordinary FEM model, crack propagation problems can be analyzed.

3. SIMULATION OF PEELING TEST

Figure 5 shows the peeling test to be analyzed by the proposed method. Two elastic plates are bonded. Young's modulus E and Poisson's ratio ν of the plate are assumed to be 3 GPa and 0.3, respectively. The computed load-displacement curves are shown in Figs. 6-9. The computed results show that the crack starts to propagate at the maximum load. Then, the load gradually decreases with increase of the peeling length. Figures 6 and 7 show the effect of material constants r_0 and n. It is indicated that the force at the start of crack extension becomes large when r_0 is small or n is large.

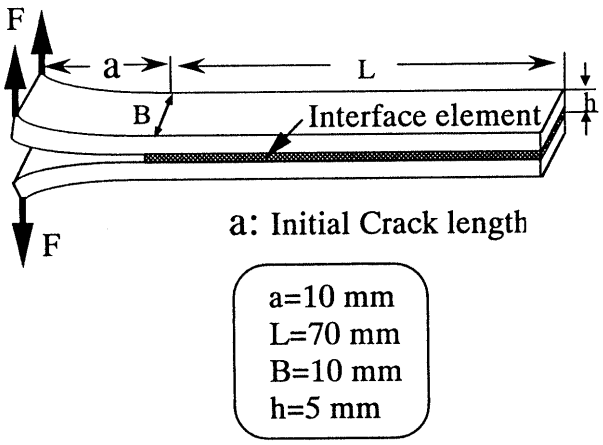

Fig. 5. Peeling test model for FEM analysis.

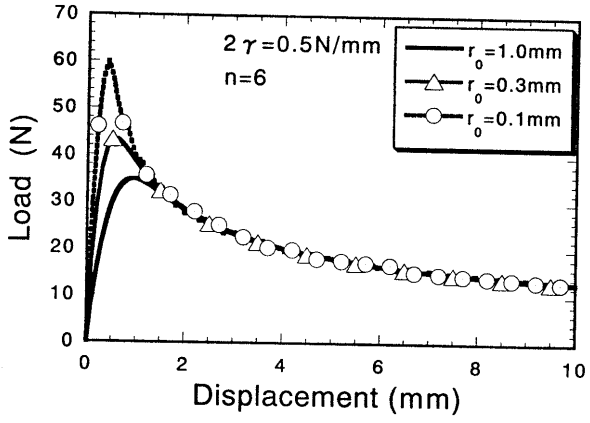

Fig. 6. Effect of r_0 on load-displacement curve.

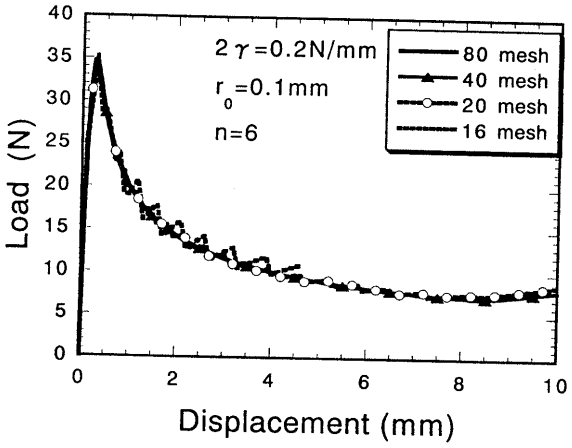

Fig. 9. Effect of mesh division on load-displacement curve.

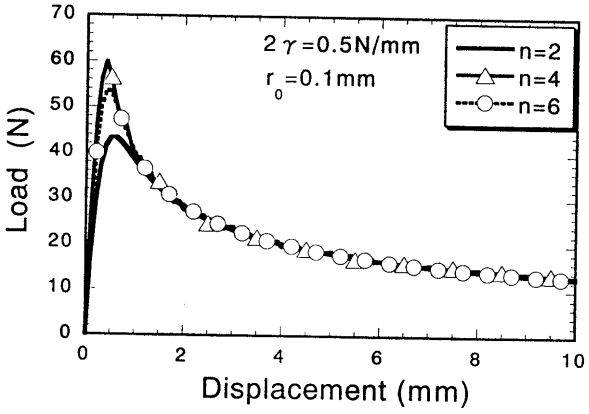

Fig. 7. Effect of n on load-displacement curve.

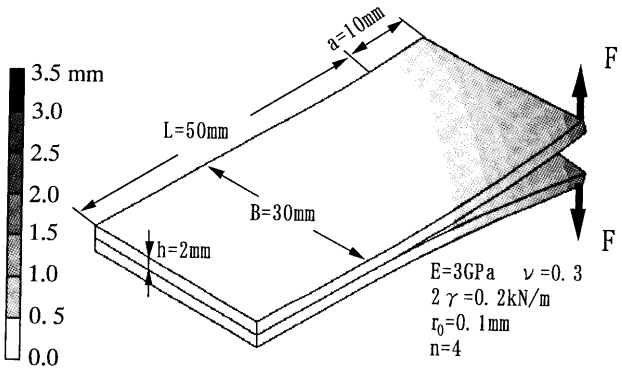

Fig. 10. Deformation of wide bonded plates under peeling.

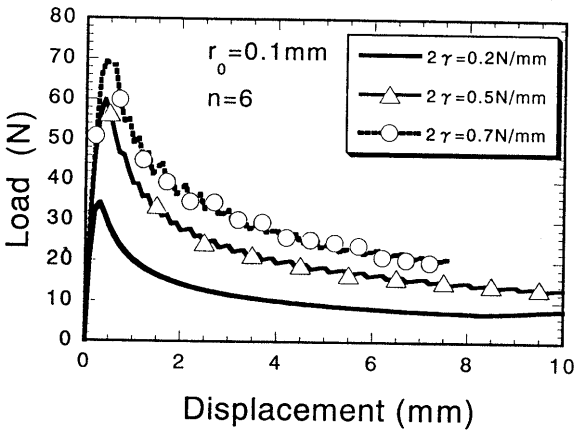

Fig. 8. Effect of γ on load-displacement curve.

On the contrary, the curve for the crack propagation process is not influenced by r_0 or n. Figure 8 shows that the value of γ influences both the initiation and the extension of the crack. These results suggest that the crack extension in peeling test is primarily governed by the magnitude of the surface energy γ. Thus, the value of γ can be estimated from the propagation part of the measured load-displacement curve and those for r_0 and n can be estimated from the point where the crack start to grow.

The effect of the mesh size is examined by changing the mesh divisions along the length of the model. As seen from Fig. 9, the mesh size does not have significant effect on the load-displacement curve. Further, peeling problem of wider plates as shown in Fig. 10 is simulated to demonstrate the potential versatility of the proposed method.

4. PUSH-OUT TEST OF FIBER IN MATRIX

The proposed method can be applied also to a mode-II crack propagation problem by replacing the opening displacement δ in Eq. (1) with the shear deformation. The push-out test of fiber in matrix shown in Fig. 11 is analyzed. In this model, the interface elements are arranged along the interface between the fiber and the matrix. The computed load-displacement curves are presented in Fig. 12. Nearly horizontal part after the linear stage corresponds to the crack propagation process. This means the load is almost constant during the crack propagation. The sudden drop of the load observed in the case of 2γ=0.2 N/mm is the moment when the interface crack reaches the bottom surface of the matrix.

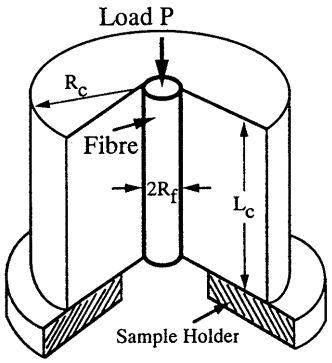

R_f Radius of fibre
R_c Radius of composite
L_c Height of composite
R_f=5 μm R_c=60 μm
L_c=80 μm
E_f=500GPa ν_f=0.01
E_c=150GPa ν_c=0.2

Fig. 11. Model for push-out test of fiber in matrix.

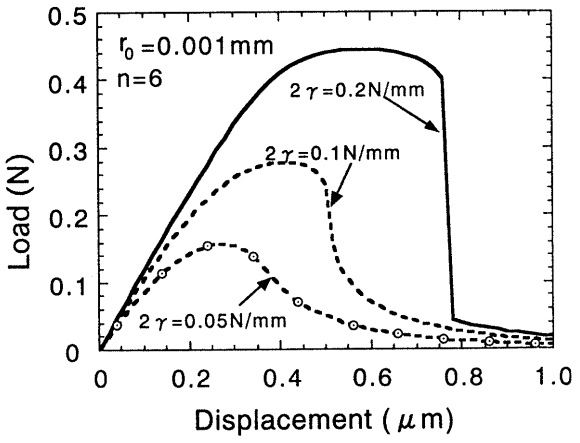

Fig. 12. Load-displacement curve of push-out test.

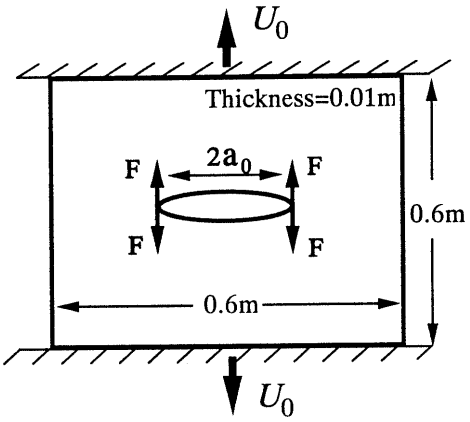

a_0=0.06 m
E=210 GPa
ν=0.3
ρ=7.85×10^3 kg/m^3
γ=50 kN/m
r_0=0.05 mm
n= 3

Fig. 13. Model for dynamic crack propagation.

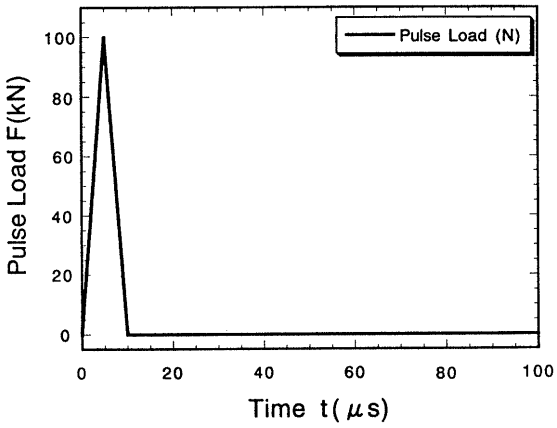

Fig. 14. Pulse load to initiate crack propagation.

5. DYNAMIC CRACK PROPAGATION

In many cases, the fracture problems are dynamic phenomena. The dynamic crack propagation in an elastic plate as shown in Fig. 13 is analyzed to demonstrate the potential capability of the proposed method. The plate has an initial crack with its length of 400 mm and it is pre-stressed by the forced displacement at the top and the bottom edges. The crack is initiated by a pulse load applied at the tip of initial crack. The pulse load in-

creases and decreases linearly in 10 μs as shown in Fig. 14. The time histories of crack extension lengths Δa for different values of pre-stress displacement U_0 are plotted in Fig. 15. As theoretically predicted [7], the speed of crack propagation increases with the value of pre-stress. When the pre-stress is small as in the case of U_0=0.4 mm, the crack is arrested. Figure 16 shows the crack extension and the distribution of stress normal to the crack at 60 and 100 μs after the application of pulse load. Due to the symmetry, only right half of the plate is shown. As it is seen, the stress wave is traveling ahead of the propagating crack.

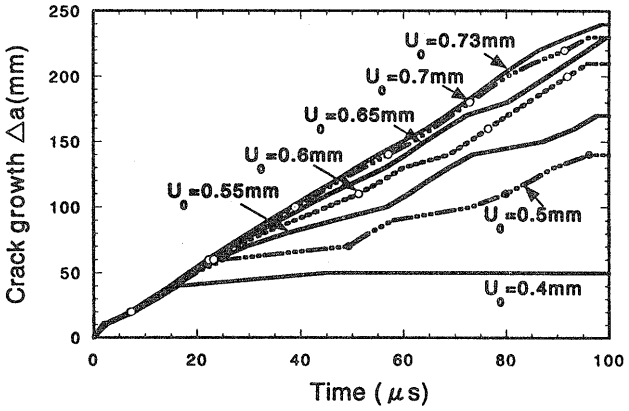

Fig. 15. Influence of pre-stress on crack propagation length.

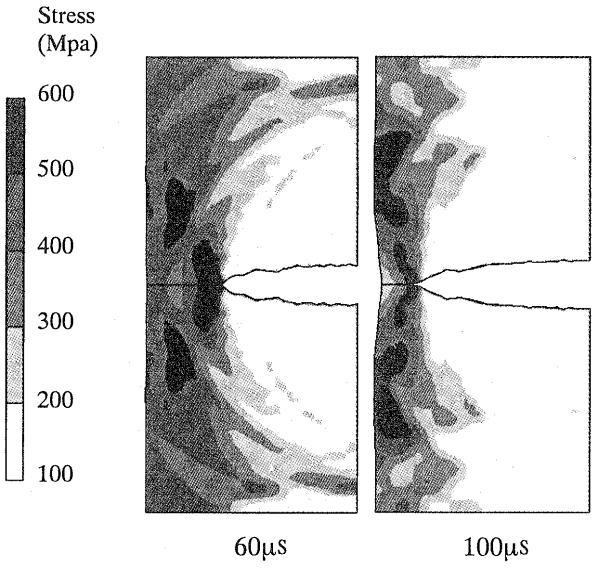

Fig. 16. Deformation and stress distribution during crack propagation.

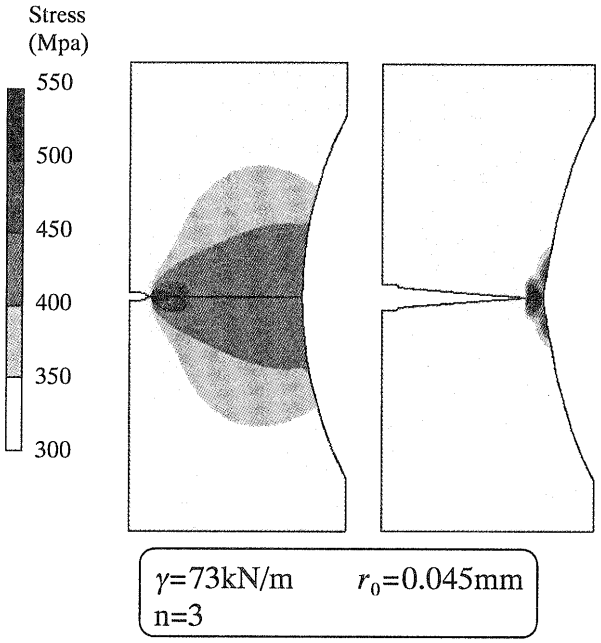

Fig. 17. Deformation and stress distribution in tearing test.

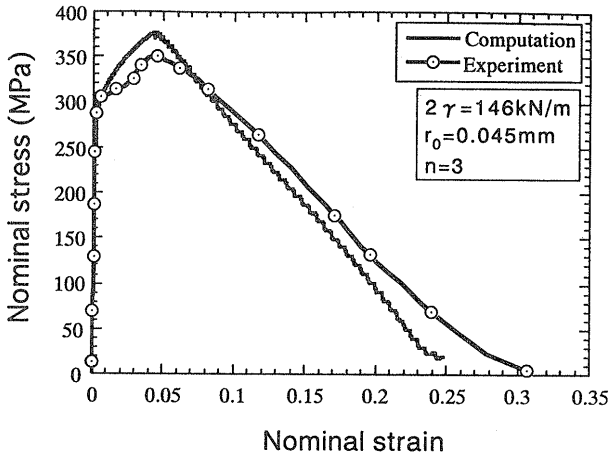

Fig. 18. Comparison with experiment.

6. DUCTILE TEARING OF STEEL PLATE

The process of tearing of steel plate with an initial notch at its center is analyzed as elastic-plastic finite strain problem using the proposed method. The length of the initial notch in the steel plate is 20 mm. The width of the plate at the central section and the thickness are 200 mm and 4.5 mm, respectively. The material is assumed to have the strain hardening property described by the following equation.

$$\sigma_Y = \sigma_{Y0}(1+\alpha\varepsilon^p)^N \ . \qquad (19)$$

where

σ_{Y0}=280 Mpa, α=115, N=0.2, E=210 Gpa, ν=0.3

The computed deformation and the distribution of the stress component in the loading direction before the crack propagation and at the final stage are presented in Fig. 17. The curves for nominal stress-strain relation are compared between FEM analysis and experiment in Fig. 18. The indicated strain is the average strain for the 50 mm gauge length at the center. Good correlation between the computation and the experiment proves the potential capability of the proposed method for the analysis of ductile crack propagation.

7. CONCLUSIONS

In order to analyze the crack propagation or the peeling, a new computer simulation method using the interface element is proposed and applied to peeling test of bonded plates, push-out test of fiber in matrix, dynamic crack in pre-stressed plate and ductile tearing of steel plate. The conclusions are as follows.

(1) The processes of mode-I or II crack propagation can be simulated by the proposed method.

(2) In the simulation of peeling test, the material constants r_0 and n influence the load at the beginning of crack propagation. However they do not have influence on the processes of crack propagation. On the other hand, γ influences both the beginning and the processes of crack propagation. The effect of mesh division on the crack propagation is found to be small.

(3) The dynamic crack propagation in a pre-stressed elastic plate is simulated and the relation between the crack propagation speed and the pre-stress is clarified.

(4) Good correlation with experiment proves the potential capability of the proposed method to ductile fracture problems.

REFERENCES

1. H. Noguchi et al., Trans. Japan Society of Mechanical Engineers, Ser. A, **63** (1997) 725 (in Japanese).
2. L. Xia and F. Shih, J. Mech. Phys. Solids., **43** (1995) 233.
3. L. Xia and F. Shih, J. Mech. Phys. Solids., **43** (1995) 1953.
4. L. Xia, F. Shih and J.W. Hutchinson, J. Mech. Phys. Solids., **43** (1995) 389.
5. H. Murakawa and Z.Q. Wu, Proc. of the Kansai Society of Naval Architects, **10** (1998) 125 (in Japanese).
6. A. Rahman, Phys. Rev., **136** (1964) 405.
7. N.F. Mott, Engineering , **165** (1948) 16.